Available online at http://scik.org
Commun. Math. Biol. Neurosci. 2020, 2020:68
https://doi.org/10.28919/cmbn/4911
ISSN: 2052-2541

IMPACT STUDIES OF NATIONWIDE MEASURES COVID-19 ANTI-PANDEMIC: COMPARTMENTAL MODEL AND MACHINE LEARNING

MOUHAMADOU A.M.T. BALDÉ[1,*], COURA BALDÉ[2], BABACAR M. NDIAYE[1]

[1]Laboratory of Mathematics of Decision and Numerical Analysis (LMDAN), Department of Mathematics of Decision(DMD)-FASEG, University of Cheikh Anta Diop, BP 45087, 10700, Dakar, Senegal

[2]Laboratory of Applied Mathematics (LMA)-FST, University of Cheikh Anta Diop, BP 45087, 10700, Dakar, Senegal

Abstract. In this paper, we deal with the study of the impact of nationwide measures COVID-19 anti-pandemic. We drive two processes to analyze COVID-19 data considering measures. We associate level of nationwide measure with value of parameters related to the contact rate of the model. Then a parametric solve, with respect to those parameters of measures, shows different possibilities of the evolution of the pandemic. Two machine learning tools are used to forecast the evolution of the pandemic. Finally, we show comparison between deterministic and two machine learning tools.

Keywords: COVID-19; nationwide measures analysis; fitting; forecasting; machine learning; asymptomatic; symptomatic.

2010 AMS Subject Classification: 92D30, 92D25, 92B20, 97R40.

1. INTRODUCTION

The COVID-19 pandemic is testing the entire world so that measures are being taken in most nations to stem its development. These measures can generally be of different kinds such as

*Corresponding author

E-mail address: mouhamadouamt.balde@ucad.edu.sn

Received August 4, 2020

social distancing, partial or total confinement, etc. It would therefore be interesting to be able to effectively analyze the effects of the measures taken on the spread of the pandemic. Here we offer an analysis of the impact of the measures taken that we apply to the case of Senegal. In previous papers [3], [11] and [12] we proposed a start of study using the results of [9].

In [9], a useful method for the study of the evolution of COVID-19 pandemic has been resented by using a compartmental model with Susceptible, Infected asymptomatic, Infected reported symptomatic and unreported symptomatic (SIRU). In [3], the author use that method to study the COVID-19 spread in Senegal with a classical SIR model.

In this work we aim to analyze the impact of the anti pandemic measures taken in Senegal. It is a continuation of the work done in [3]. We do a two-step analysis. The first uses the differential equations model denoted SIRU introduced in [9], and the second uses two machine learning tools: Predict of Wolfram Mathematica using Neural Networks method and Prophet.

We conduct the work in the following way. In the section 2 we study the effect of the nationwide measures by using an epidemic model presented in [9] and we present some machine learning tools. We show, in the section 3, the numerical results. In the section 4, we discuss the results. Then in section 5, we perform an analysis of the model and explain the parameters estimation. Finally in the section 6, we end by making a conclusion and advancing perspectives.

2. ANALYSIS

2.1. Analysis of the measures. In [3] a classical SIR model was studied using results from the paper [9]. The aim was to analyze the effect of the nationwide measures using the data after nationwide measures. In fact, throughout t_0 to T, we fitted an exponential function to the data of the total cases of infection of this period. T represents the date of the nationwide measures, and t_0 is the starting time of the epidemic. We consider that the effects of the measures are such that they lead to a reduction in the contact rate. To describe this reduction, we chose a slowly decreasing function over time. We consider that the measures taken are not strong enough to systematically drop the contact rate to 0. This new function corresponds to the first one and the data in the period before measures from t_0 to T, then takes a slower trajectory than that of the first function after T. In other words, from the date T, the new curve goes under the old one. We consider that if on the dates $t > T$ the data goes under the new curve obtained with a contact

rate after measures then, we can say that these measures affect the evolution of the pandemic. In the previous paper [3], the function we fitted to the data from 2020 March 02 to March 31 by least square method, is $TNI(t) = b\exp(ct) - a$ with $a = 13.9324,\ b = 9.61779$ and $c = 0.100095$ (figure 1a). In this paper we fit a new exponential function to the data from 2020 March 02 to April 25 (figure 1b). For this new function, we have $a = 99.9214,\ b = 81.325,\ c = 0.0371767$.

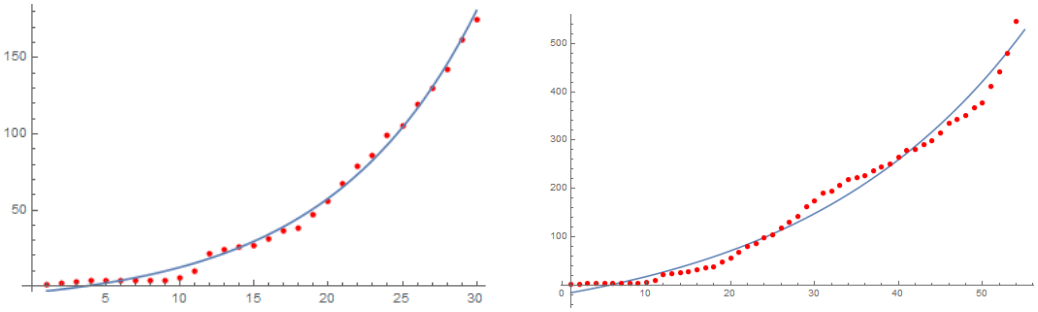

(A) Fit with data of the total cases: $TNI(t)$ is the blue line and the data are the red dotted. From 2020 March 02 to March 31.

(B) Fit with data of the total cases: $TNI(t)$ is the blue line and the data are the red dotted. From 2020 March 02 to April 25.

FIGURE 1. Plot of the exponential curves fitting the total number of case Senegal's data.

To continue in our analysis, we will use a differential equations model introduced in [9]. This model is as follows:

$$(1)\qquad \begin{cases} \dfrac{dS}{dt} = -\beta S(t)(I(t) + I_U(t)) \\ \dfrac{dI}{dt} = \beta S(t)(I(t) + I_U(t)) - \nu I(t) \\ \dfrac{dI_R}{dt} = \gamma\nu I(t) - \eta I_R(t) \\ \dfrac{dI_U}{dt} = (1-\gamma)\nu I(t) - \eta I_U(t) \end{cases}$$

The initial conditions are $S(t_0) = S_0 \geq 0$, $I(t_0) = I_0 \geq 0$ $I_R(t_0) = I_{R0} \geq 0$, and $I_U(t_0) = I_{U0} \geq 0$ and t_0 the initial time of the epidemic. With $S(t)$ represents the susceptible individuals, I the infected asymptomatic individuals, I_U the unreported infected symptomatic and I_R the reported infected symptomatic individuals.

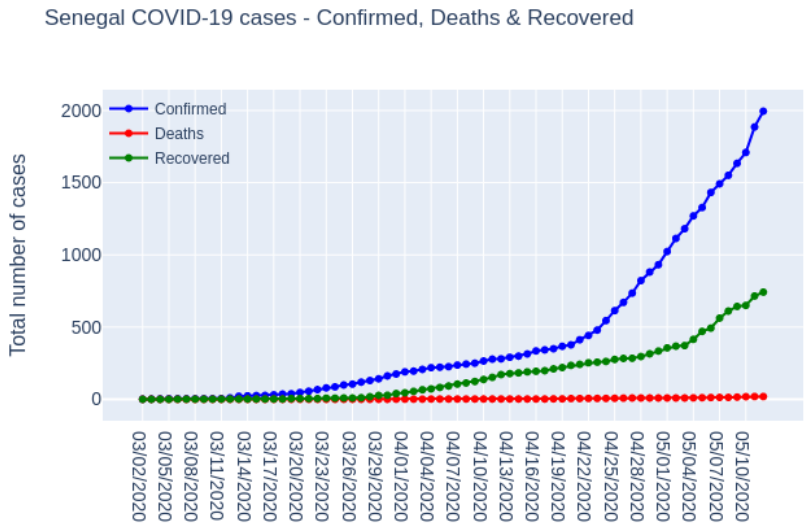

FIGURE 2. Plot of data of total confirmed, death and recovered from 2020 March 02 to May 10.

We can also consider a version with removed compartments, the recovered R and the death D:

$$
(2) \qquad \begin{cases} \dfrac{dS}{dt} = -\beta S(t)(I(t)+I_U(t)) \\ \dfrac{dI}{dt} = \beta S(t)(I(t)+I_U(t)) - \nu I(t) \\ \dfrac{dI_R}{dt} = \gamma\nu I(t) - \eta I_R(t) \\ \dfrac{dI_U}{dt} = (1-\gamma)\nu I(t) - \eta I_U(t) \\ \dfrac{dR}{dt} = \alpha\eta(I_R(t)+I_U(t)) \\ \dfrac{dD}{dt} = (1-\alpha)\eta(I_R(t)+I_U(t)) \end{cases}
$$

Let's present the parameters. β is the contact rate. $1/\nu$ is the average time during which asymptomatic infectious are asymptomatic. γ is the fraction of asymptomatic infectious individuals that become reported symptomatic infectious. $1/\eta$ is the average time symptomatic infectious have symptoms. $\gamma\nu$ is the rate at which asymptomatic infectious become reported symptomatic. $(1-\gamma)\nu$ is the rate at which asymptomatic infectious become symptomatic but unreported. α is the proportion of recovered and $1-\alpha$ is the proportion of death due to the infection.

We make the assumption that the function we fit the total number of reported infected cases is given by $\gamma\nu \int_{t0}^{t} I(s)ds$.

The starting time of the pandemic, the initial conditions and some parameters of the model are estimated and others are fixed. The parameters set are γ, $1/\nu$ and $1/\eta$. The values chosen for $1/\nu$ and $1/\eta$ are those used by the medical authorities i.e. $1/7$. Regarding the proportion of unreported and reported, we also use the same value proposed in [9], ie 80% are reported and 20% are unreported. Further detailed studies could make it possible to estimate the good value of this proportion for Senegal where we apply the model. For the estimation of the parameters, the starting time and the initial conditions, we use the calculation methods detailed in [9] and [3].

We start with the fitting exponential function which we equalize with the integral formula above $TNI(t) = b\exp(ct) - a = \gamma\nu \int_{t0}^{t} I(s)ds$. Hence some calculation of derivations, replacement in the model and integration gives:

- $t_0 = \dfrac{ln(a) - ln(b)}{c}$.
- $I(t) = I(t_0)\exp(c(t-t_0))$, with $I(t_0) = I_0 = \dfrac{ac}{\gamma\nu}$.
- $I_U(t) = I_U(t_0)\exp(c(t-t_0))$, with $I_U(t_0) = I_{U0} = \dfrac{(1-\gamma)ac}{\gamma(\eta+c)} = \dfrac{(1-\gamma)\nu}{\eta+c} I_0$.
- $I_R(t) = I_R(t_0)\exp(c(t-t_0))$, with $I_R(t_0) = I_0 - I_{U0} = \dfrac{ac}{\eta+c} = \dfrac{\gamma\nu}{\eta+c} I_0$.
- $R(t) = \dfrac{\alpha\eta\nu(I(t)-I_0)}{c(c+\eta)}$.
- $D(t) = \dfrac{(1-\alpha)\eta\nu(I(t)-I_0)}{c(c+\eta)}$.
- $\beta = \dfrac{c+\nu}{S_0}\dfrac{\eta+c}{(1-\gamma)\nu+\eta+c}$.
- $\mathscr{R}_0 = \dfrac{c+\nu}{\nu}\dfrac{\eta+c}{(1-\gamma)\nu+\eta+c}(1+\dfrac{(1-\gamma)\nu}{\eta})$.

For more details see section 5.

We consider that after the measures taken at the time T, the contact rate depends on time following a formula we choose. We use two formulas. One of them was introduced in [3], and the second one was proposed in [10]. The first one is :

$$\tilde{\beta}(t) = \begin{cases} \beta & \text{if } t \in [t_0,\ T] \\ \beta(\dfrac{T}{t})^{\delta/p} & \text{if } t > T, \end{cases} \tag{3}$$

where δ and p are parameters to choose. The second one is:

$$\tilde{\beta}(t) = \begin{cases} \beta & \text{if } t \in [t_0,\ T] \\ \beta\exp(-\varphi(t-T)) & \text{if } t > T, \end{cases} \tag{4}$$

where φ is a parameter to choose.

Then the new model to solve is:

$$
(5) \qquad \begin{cases} \dfrac{dS}{dt} = -\tilde{\beta} S(t)(I(t) + I_U(t)) \\ \dfrac{dI}{dt} = \tilde{\beta} S(t)(I(t) + I_U(t)) - \nu I(t) \\ \dfrac{dI_R}{dt} = \gamma \nu I(t) - \eta I_R(t) \\ \dfrac{dI_U}{dt} = (1-\gamma)\nu I(t) - \eta I_U(t) \end{cases}
$$

By solving (5), we get $\tilde{I}(t)$ from which we can calculate the total number of infected with the formula $T\tilde{N}I(t) = \gamma\nu \int_{t0}^{t} \tilde{I}(s)ds$. We choose values of parameters of $\tilde{\beta}$ such that $T\tilde{N}I(t)$ follows the same path that $TNI(t)$. Then, by way of parameters δ and p in $\tilde{\beta}$, we can evaluate the measures. We do parametric solve with respect to parameters δ and p. Results are shown in figure 5.

Now we consider at time T_2, the nation applies stronger measures. We simply interpret as the contact rate $\tilde{\beta}$ is reduced by a factor $\phi \in [0,1]$. When the value of ϕ is equal to 0, it means that there are no measures, while when ϕ is equal to 1, it means that the strongest measures are taken. Hence the measures are quantified with the values of proportion ϕ. Then the contact rate become:

$$
(6) \qquad \tilde{\beta}_2(t) = \begin{cases} \tilde{\beta}(t) & \text{if } t \in [t_0,\ T_2] \\ (1-\phi)\tilde{\beta}(T_2) & \text{if } t > T_2, \end{cases}
$$

We solve the new model with $\tilde{\beta}$ replaced by $\tilde{\beta}_2$. We do a parametric solve with respect to the parameter ϕ, and we plot the result for different values of ϕ. Then, we show different values of the peak, depending on the values of ϕ. Then, we can evaluate the maximal value of infection peak with respect to the level of the measures. Results are shown in figures 6, 7, 8 and 9.

2.2. Artificial Neural Networks. Artificial neural networks are part of artificial intelligence. Biological neural networks inspire them. Biological neural networks are part of the animal

brain. One of the main functions of the brain is to process information, and the primary information processing element is the neuron. This specialized brain cell combines (usually) several inputs to generate a single output. Depending on the animal, an entire brain can contain anywhere from a handful of neurons to more than a hundred billion, wired together. The output of one cell feeding the input of another, to create a neural network capable of remarkable feats of calculation and decision making (See [13]). If we could qualify the brain as a computer, then we would say that it is the best of computers. For this reason, the engineer seeks to improve mechanical computers to be closer to the biological computer, i.e., the brain. The more neural connections there are, the more the network can solve complex problems. Pattern recognition is a task that neural networks can easily accomplish. For this task, introducing as input a pattern to a neural network, yields as output a pattern back (See [5]).

In general, neural network problems involve a dataset used to predict values for later datasets. For that, the neural network needs to be trained. Then, neural networks can predict the outcome of entirely new datasets based on training from old data sets.

Most neural network structures use some type of neuron, node, or unit. An algorithm called a neural network will generally be made up of individual interconnected neurons, see figure 3.

The artificial neuron receives input from one or more sources, which may be other neurons or data entered into the network from a computer program see figure 4. This entry is usually a floating-point or binary. Often the binary input is coded floating point representing true or false like 1 or 0. Sometimes the program also describes the binary input as using a bipolar system with true as 1 and false as -1. An artificial neuron multiplies each of these inputs by a weight. It then adds these multiplications and transmits this sum to an activation function given by:

$$f(x_i, w_i) = \phi\left(\sum_{i=1}^{n}(w_i \cdot x_i)\right), \tag{7}$$

with the variables x and w represent the input and the weights of the neuron, n is the number of input and weight.

Some neural networks do not use an activation function. To read more about Neural Networks one can see [1], [5], [4] and [13].

Neural networks are implemented in machine learning tools of many software like Wolfram Mathematica[18]. We use the machine learning tool "Predict" to forecast the evolution of the COVID-19 pandemic in Senegal. We can choose different method of regression algorithm: "RandomForest", "LinearRegression", "NeuralNetwork", "GaussianProcess", "NearestNeighbors", etc.

We use the "NeuralNetwork" regression algorithm, which predicts using artificial neural networks.

We consider two cases in the forecasting. The first case, only use the total number of infected case data in the training of the neural networks. While in the other forecasting, we use two types of data: the total number of infected cases and the contact rate. In the second case, the aim is to do forecasting by considering the effect of the contact rate. It is a way to show the effect of the nationwide measures taken at the time T, as specified in section 2. For the contact rate we use as data $\tilde{\beta}$ given by (3).

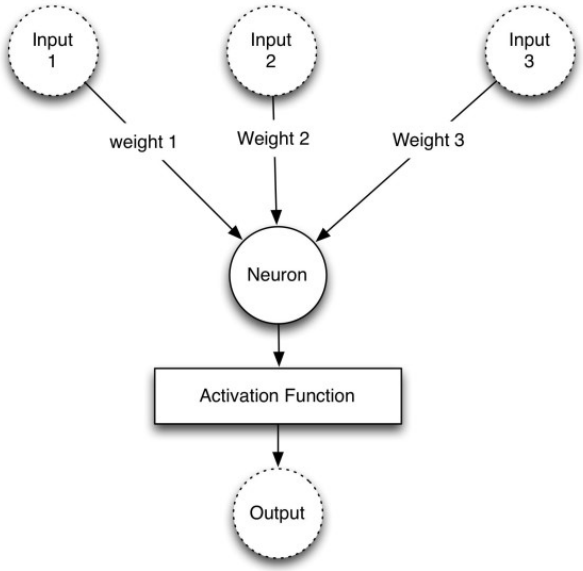

FIGURE 3. Example of artificial neuron from [5].

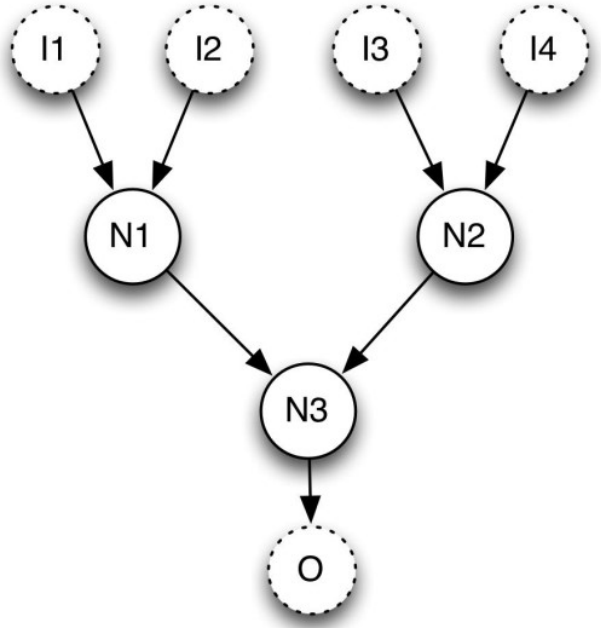

FIGURE 4. Example of artificial neural networks from [5]. I1, I2 and I3 mean input 1,2 and 3. N1, N2 and N3 mean neuron 1,2 and 3. O means output.

2.3. Forecasting using Prophet. In this section, we develop another machine learning tool for forecasting to compare with the previous SIRU models and Neural Networks method.
We use Prophet [15], a procedure for forecasting time series data based on an additive model where non-linear trends are fit with yearly, weekly, and daily seasonality, plus holiday effects.
For the average method, the forecasts of all future values are equal to the average (or "mean") of the historical data. If we let the historical data be denoted by $y_1,...,y_T$, then we can write the forecasts as

$$\hat{y}_{T+h|T} = \bar{y} = (y_1 + y_2 + ... + y_T)/T$$

The notation $\hat{y}_{T+h|T}$ is a short-hand for the estimate of y_{T+h} based on the data $y_1,...,y_T$. A prediction interval gives an interval within which we expect y_t to lie with a specified probability. For example, assuming that the forecast errors are normally distributed, a 95% prediction interval for the h-step forecast is

$$\hat{y}_{T+h|T} \pm 1.96\hat{\sigma}_h$$

where σ_h is an estimate of the standard deviation of the h-step forecast distribution.
For the data preparation, when we are forecasting at the country level, for small values, forecasts

can become negative. To counter this, we round negative values to zero. Also, no tweaking of seasonality-related parameters and additional regressors are performed.

3. NUMERICAL SIMULATIONS

3.1. Numerical analysis. The data for Senegal, we use, is obtained from daily press releases on the COVID-19 from the Ministry of Health and Social Action (`http://www.sante.gouv.sn/`).

The figures 6, 7, 8 and 9 show results related to 2.1. The figures 6, 7 correspond to $\tilde{\beta}$ 3 and the figures 8, 9 correspond to $\tilde{\beta}$ 4.

We use $\gamma = 0.8,\ \nu = 1/7,\ \eta = 1/7$, the total population of Senegal is $N = 16743927$ from Senegal Population (2020) - Worldometer (www.worldometers.info). Then we obtain: $t_0 = 5.53923,\ I_0 = 32.504,\ I_{U0} = 5.1584,\ I_{R0} = 27.3456,\ S_0 = N - I_0 = 1.67439 \times 10^7,\ \mathscr{R}_0 = 1.30516$, $\beta = 9.27954 \times 10^{-9}$.

The time of the nationwide measures in Senegal taken at 2020, March 23 is considered. Then $T = 23$. For $\tilde{\beta}$ given by (3), results are shown by figures 6a and 6b. For $\tilde{\beta}$ given by (4), results are shown by figures 8a and 8b. We see that the maximal number of reported case goes up to 340000 with the time peak at $t = 310$, which correspond to 2021, January 05.

A parametric plot of a parametric resolution of the SIRU model (5), using $\tilde{\beta}$ given by (3), with respect to δ and p, is shown in figures 5.

Now, we consider that stronger measures is taken as explained in the subsection 2.1. The results is shown in figures 6c, 8c, 6d, 8d, 6e, 8e, 6f, 8f and 7.

Particularly figure 6c and figures 8c shows results of parametric solve of the SIRU model (5) with the parameters $\phi = 0$. Hence, we see that the time of the peak becomes T_2, the date where stronger measures are taken. We choose as sample $T_2 = 70$ which correspond to 2020, May 10.

The figures 6d, 8d, 6e, 8e, 6f, 8f show parametric plot of the infected $I(t)$, the reported $I_R(t)$ and unreported $I_U(t)$ and total number of infected $T\tilde{N}I(t)$, with varying values of the parameter ϕ.

The figures 7 and 9 show again, in different range of the ordinate axis, parametric plot of the infected $I(t)$, the reported $I_R(t)$ and unreported $I_U(t)$ and total number of infected $T\tilde{N}I(t)$, with varying values of the parameter ϕ.

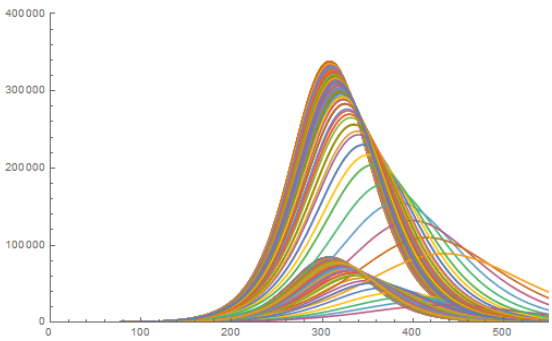

(A) Parameric plot of the reported $I_R(t)$ and unreported $I_U(t)$ infected case.

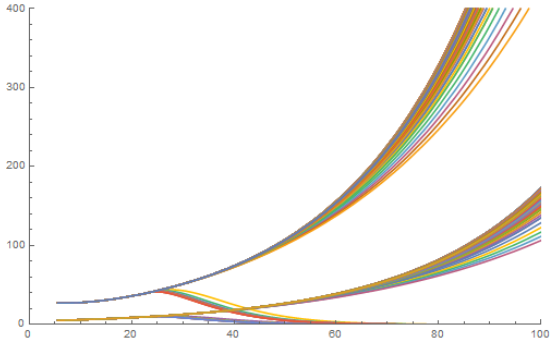

(B) Zoom of the parameric plot of the reported $I_R(t)$ and unreported $I_U(t)$ infected case.

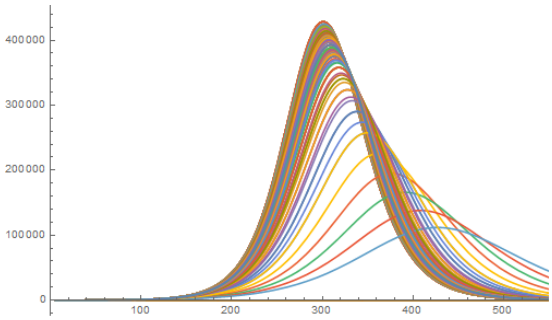

(C) Parameric plot of the infected $I(t)$.

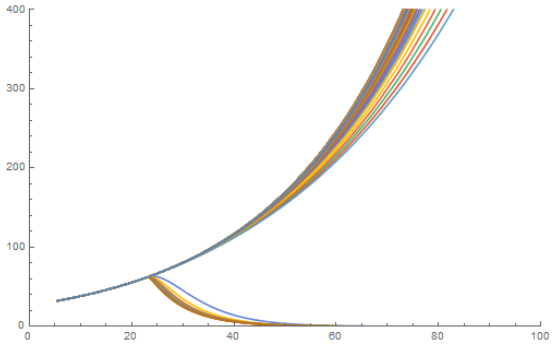

(D) Zoom of parameric plot of the infected $I(t)$.

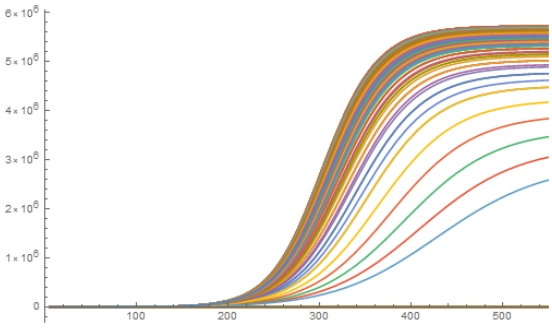

(E) Parameric plot of the total number of infected case $T\tilde{N}I(t)$.

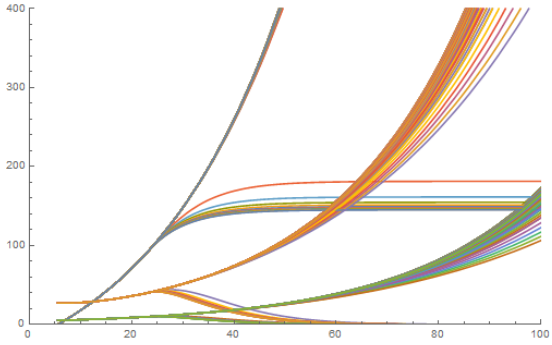

(F) zoom of the parameric plot of $T\tilde{N}I(t)$, $I_R(t)$ and $I_U(t)$.

FIGURE 5. View of different sizes parametric plot of the SIRU model(2) using (3), with measures taken at a time T. From top to down corresponding to increasing values of the parameter δ/p, with $\delta \in [0,\ 50]$ by step 5 and $p \in [1,\ 10001]$ by step of 1000. On the abscissa axis, the graduation 55 represents 2020, April 25.

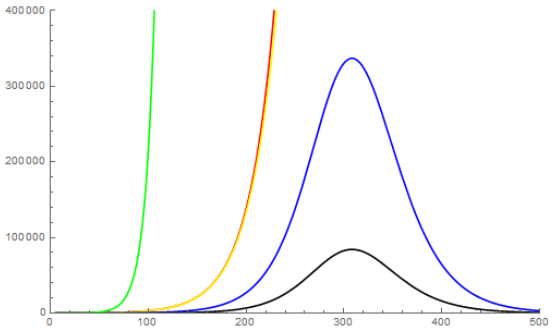

(A) $TNI(t)$ in red line, $T\tilde{N}I(t)$ in yellow, $I_R(t)$ in blue line, $I_U(t)$ in black line, the old fit function in green line.

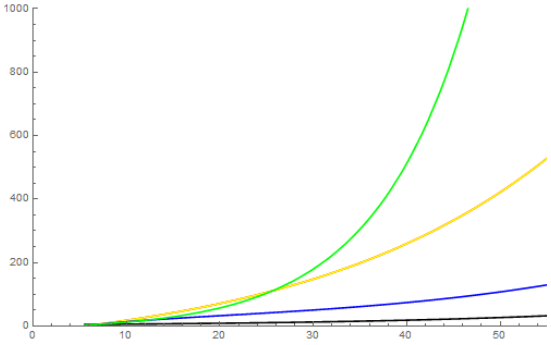

(B) Plot, with maximal ordinate value fixed to 1000. $TNI(t)$ and $T\tilde{N}I(t)$ in yellow have the same path.

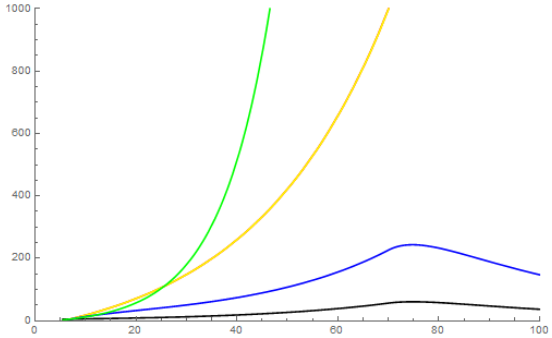

(C) Plot with stronger measures at time T_2 and $\phi = 1$.

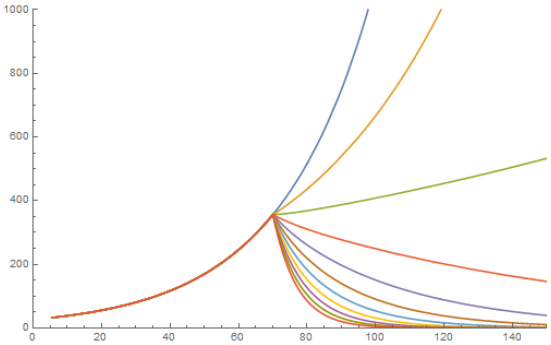

(D) Parameric plot of the infected case $I(t)$.

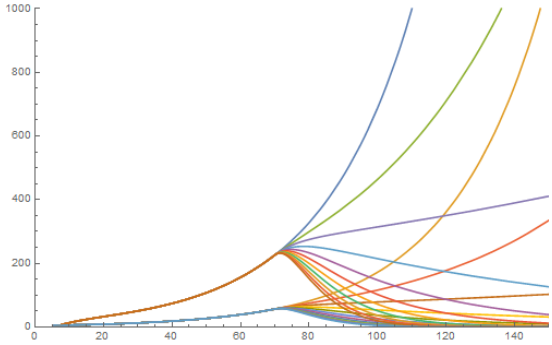

(E) Parameric plot of $I_R(t)$ and $I_U(t)$.

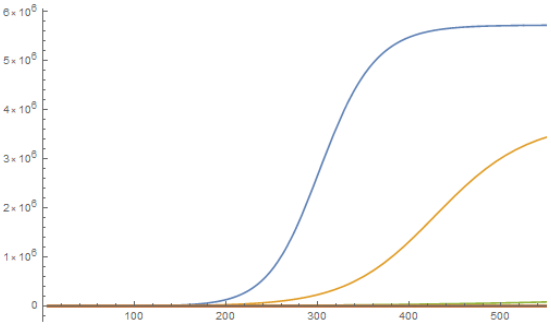

(F) Parameric plot of $T\tilde{N}I(t)$.

FIGURE 6. Plot and parametric plot of the SIRU model(2), using (3) with $\delta = 1$ and $p = 5000$ and (6) with ϕ as parameter, fitted to data of Senegal. With stronger measures taken at a time T_2. From top to down corresponding to increasing values of the parameter ϕ from 0 to 1 by step of 0.1. On the abscissa axis, the graduation 55 represents 2020, April 25.

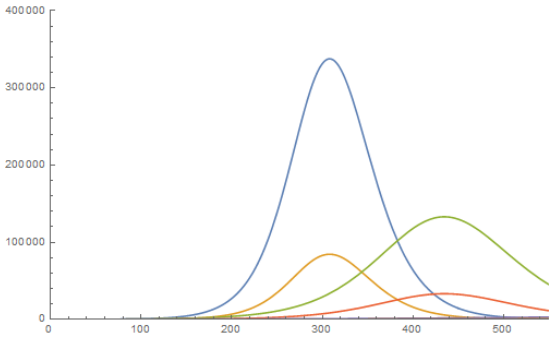

(A) Zoom of parameric plot of $I_R(t)$ and $I_U(t)$.

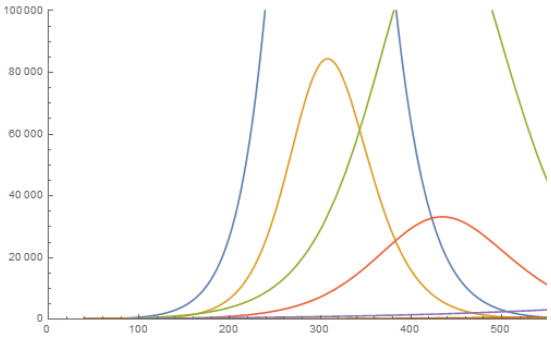

(B) Zoom of parameric plot of $I_R(t)$ and $I_U(t)$.

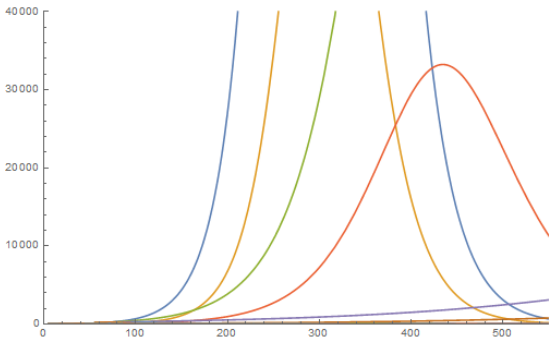

(C) Zoom of parameric plot of $I_R(t)$ and $I_U(t)$.

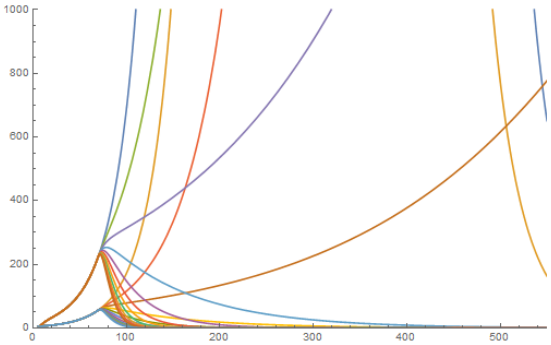

(D) Zoom of parameric plot of $I_R(t)$ and $I_U(t)$.

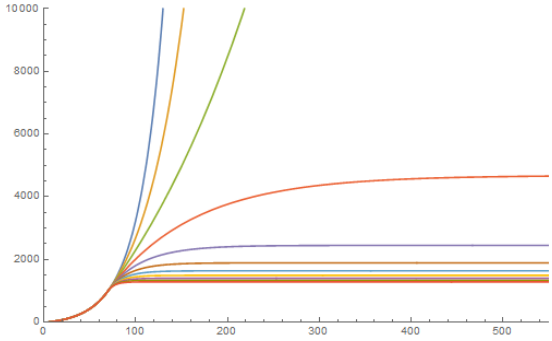

(E) Zoom of parameric plot of $T\tilde{N}I(t)$.

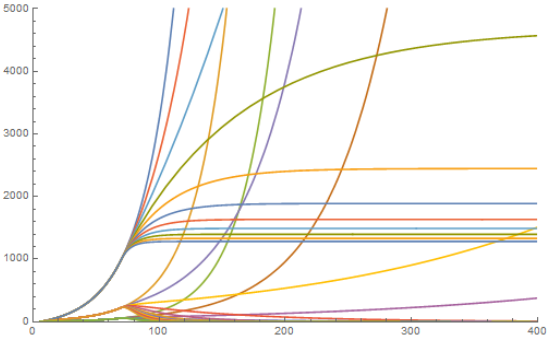

(F) Zoom of parameric plot of $T\tilde{N}I(t)$, $I_R(t)$ and $I_U(t)$.

FIGURE 7. View of different sizes parametric plot of the SIRU model(2) using (4), with stronger measures taken at a time T_2. From top to down corresponding to increasing values of the parameter ϕ from 0 to 1 by step of 0.1. On the abscissa axis, the graduation 55 represents 2020, April 25.

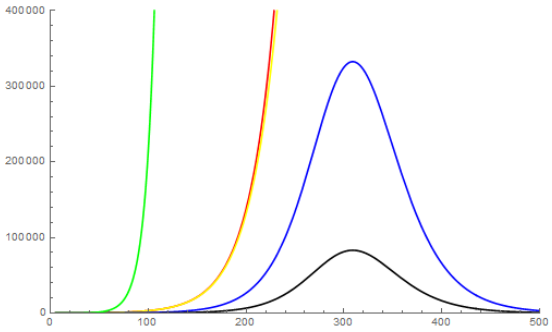

(A) $TNI(t)$ in red line, $T\tilde{N}I(t)$ in yellow, $I_R(t)$ in blue line, $I_U(t)$ in black line, the old fit function in green line.

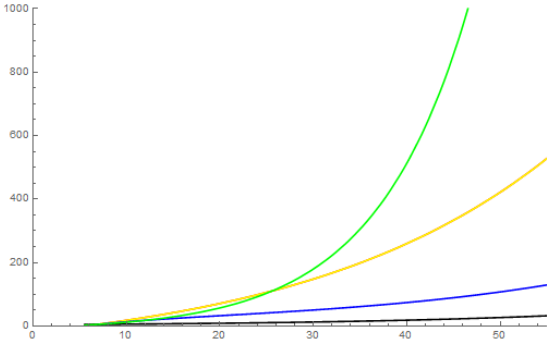

(B) Plot, with maximal value fixed to 1000. $TNI(t)$ in red line and $T\tilde{N}I(t)$ in yellow have the same path.

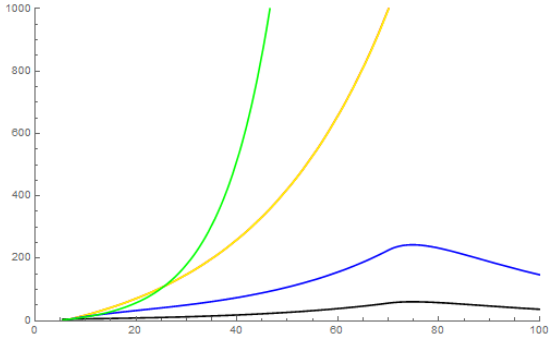

(C) Plot with stronger measures at time T_2 and $\phi = 1$.

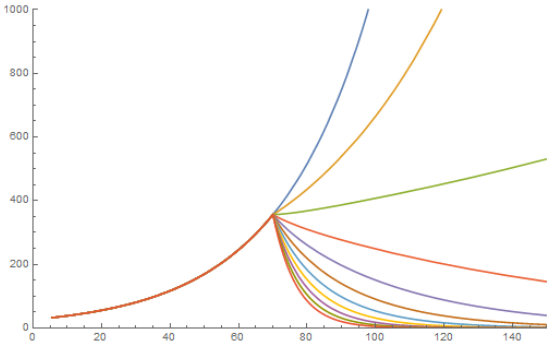

(D) Parameric plot of the infected case $I(t)$.

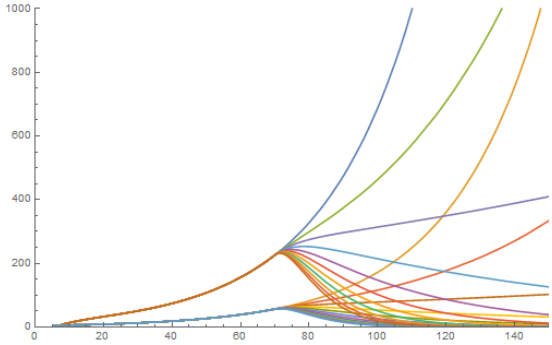

(E) Parameric plot of $I_R(t)$ and $I_U(t)$.

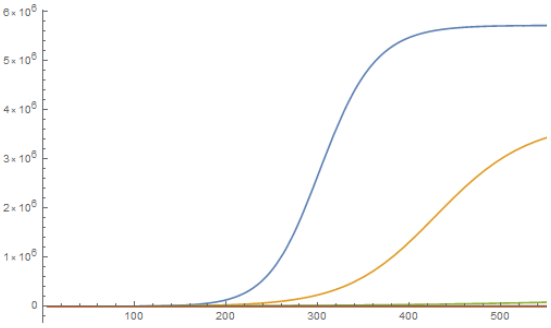

(F) Parameric plot of $T\tilde{N}I(t)$.

FIGURE 8. Plot and parametric plot of the SIRU model(2), using (4) with $\varphi = 10^{-5}$ and (6) with ϕ as parameter, fitted to data of Senegal. With stronger measures taken at a time T_2. From top to down coresponding to increasing values of the parameter ϕ from 0 to 1 by step of 0.1. On the abscissa axis, the graduation 55 represents 2020, April 25.

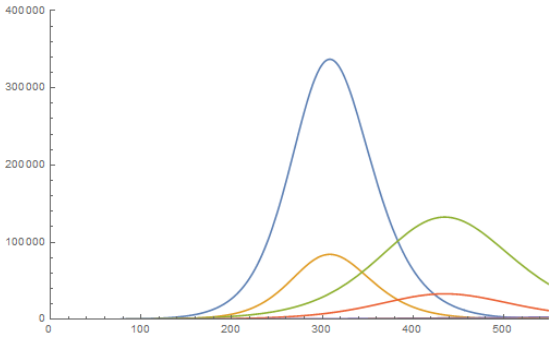

(A) Zoom of parameric plot of $I_R(t)$ and $I_U(t)$.

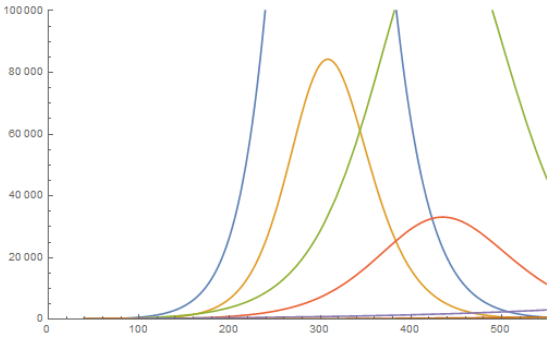

(B) Zoom of parameric plot of $I_R(t)$ and $I_U(t)$.

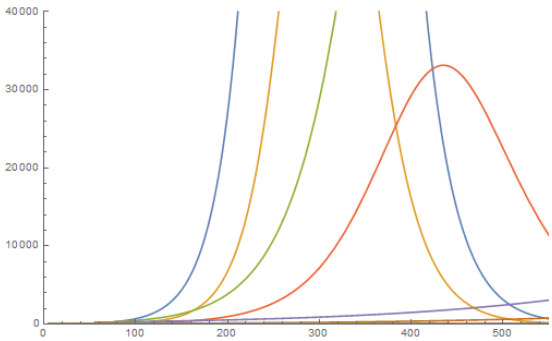

(C) Zoom of parameric plot of $I_R(t)$ and $I_U(t)$.

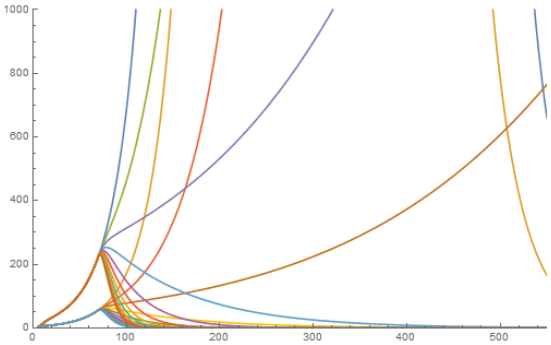

(D) Zoom of parameric plot of $I_R(t)$ and $I_U(t)$.

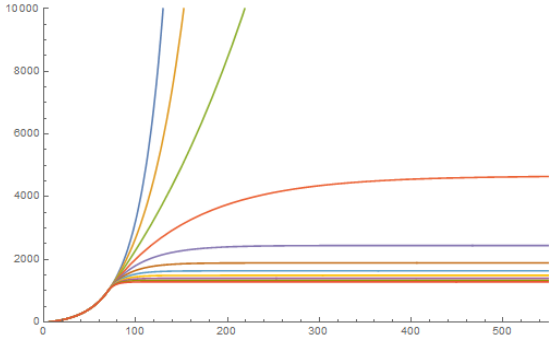

(E) Zoom of parameric plot of $T\tilde{N}I(t)$.

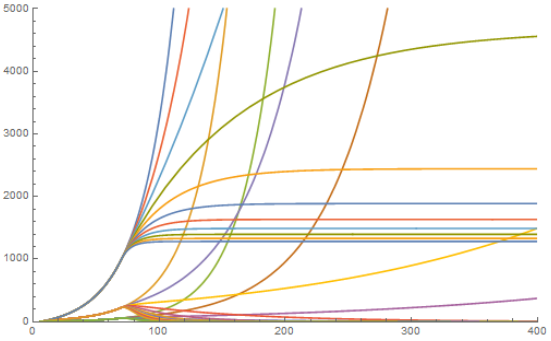

(F) Zoom of parameric plot of $T\tilde{N}I(t)$, $I_R(t)$ and $I_U(t)$.

FIGURE 9. View of different sizes parametric plot of the SIRU model(2) using (6), with stronger measures taken at a time T_2. From top to down corresponding to increasing values of the parameter ϕ from 0 to 1 by step of 0.1. On the abscissa axis, the graduation 55 represents 2020, April 25.

3.2. Comparative forecasting with machine learning. The forecasting is done with two data set. For both data from March 02, to April 25, 2020 and March 02, to May 12, 2020 we carry out simulations for a longer time and forecast the potential trends of the COVID-19 pandemic in Senegal. The predicted cumulative number of confirmed cases are first plotted for periods until May 26, June 10 and Sept. 18, 2020 ahead forecast with Prophet, with 95% prediction intervals.

The confirmed predictions for Senegal, using Prophet are given in Figure 12 (see Tables 2, 3 and 4 for the value of the confidence interval).

The figures 11 shows forecasting using Neural Networks method of Predict. Particularly the figure 11 shows two forecasting, one based only on data and an other obtained by training the Neural Networks method with data and contact rate. The prediction are done until 2020, May 26, June 10 and September 18.

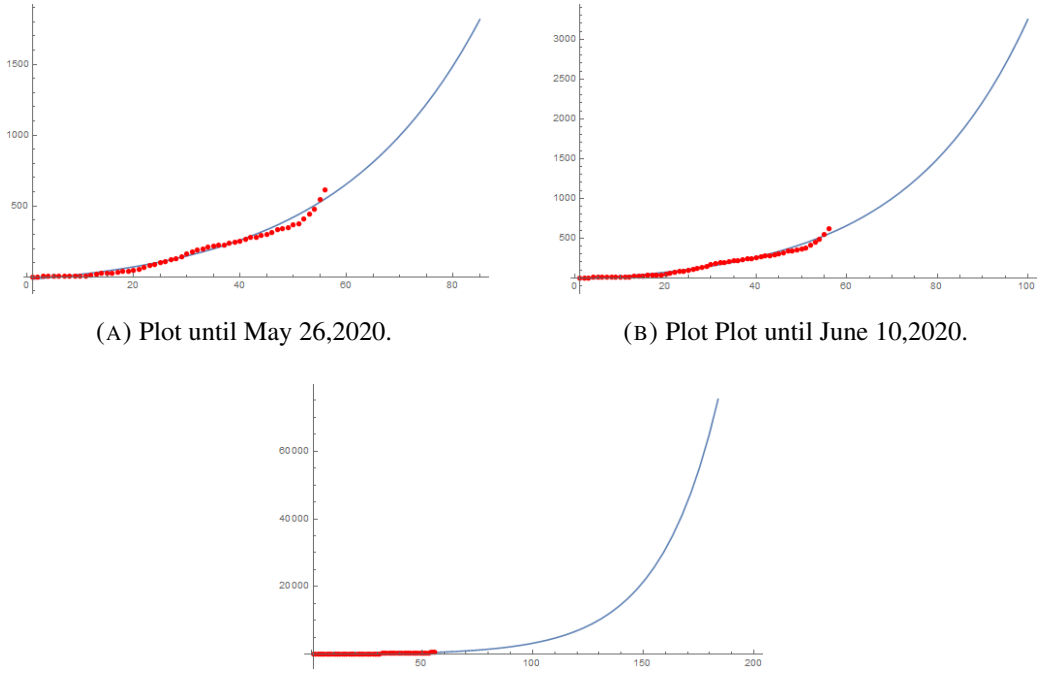

(A) Plot until May 26,2020.

(B) Plot Plot until June 10,2020.

(C) Plot until September 18, 2020.

FIGURE 10. Plot the function $TNI(t)$ in blue line with data set 1 in red dotted, until the dates 2020, May 26, June 10 and September 18 corresponding to the graduations 85, 100 and 200 on the abscissa axis.

TABLE 1. Predicted cumulative confirmed cases using SIRU model. Forecasting until the dates May 26, June 10 and September 18, 2020.

Until date J	$J-4$	$J-3$	$J-2$	$J-1$	J
J =2020-05-26	1552.118087	1614.691394	1679.634752	1747.037931	1816.9941
J =2020-06-10	2785.471575	2894.759872	3008.187615	3125.911594	3248.094533
J =2020-09-18	118687.0026	123186.2236	127855.8589	132702.3632	137732.4357

TABLE 2. Data set 2. Predicted cumulative confirmed cases ∼May 26, 2020, from top to down using Prophet and Neural Networks method of Predict. On the down, from left to right with data set & contact rate and data set only.

Date	$\hat{y}$	$\hat{y}_{lower}$	$\hat{y}_{upper}$
2020-05-22	2695.292384	2598.664351	2807.280554
2020-05-23	2777.228597	2663.535151	2897.959707
2020-05-24	2853.863973	2718.853527	2994.394743
2020-05-25	2945.018292	2802.374207	3095.868137
2020-05-26	3024.913096	2857.548751	3196.443359

Date	P^{β}	P^{β}_{lower}	P^{β}_{upper}	P	P_{lower}	P_{upper}
2020-05-22	2509.179622	2438.869281	2579.489963	2714.814079	2647.304599	2782.323560
2020-05-23	2575.632714	2505.322373	2645.943055	2803.067798	2735.558317	2870.577278
2020-05-24	2641.331365	2571.021025	2711.641706	2891.331968	2823.822488	2958.841449
2020-05-25	2706.266493	2635.956152	2776.576834	2979.590415	2912.080934	3047.099895
2020-05-26	2770.436355	2700.126014	2840.746696	3067.828454	3000.318974	3135.337935

TABLE 3. Data set 2. Predicted cumulative confirmed cases ∼June 10, 2020, from top to down using Prophet and Neural Networks method of Predict. On the down, from left to right with data set & contact rate and data set only.

Date	$\hat{y}$	$\hat{y}_{lower}$	$\hat{y}_{upper}$
2020-06-06	3887.495614	3491.259628	4284.386057
2020-06-07	3964.130990	3541.984441	4387.085352
2020-06-08	4055.285309	3616.658728	4496.788853
2020-06-09	4135.180113	3685.960670	4604.522925
2020-06-10	4206.725884	3726.064523	4685.455882

Date	P^{β}	P^{β}_{lower}	P^{β}_{upper}	P	P_{lower}	P_{upper}
2020-06-06	3409.698565	3339.388223	3480.008905	4034.675309	3967.165829	4102.184790
2020-06-07	3462.752283	3392.441942	3533.062624	4122.100051	4054.590571	4189.609532
2020-06-08	3515.229377	3444.919036	3585.539718	4209.437690	4141.928209	4276.947171
2020-06-09	3567.143036	3496.832695	3637.453377	4296.685488	4229.176007	4364.194968
2020-06-10	3618.508442	3548.198100	3688.818782	4383.845435	4316.335955	4451.354916

TABLE 4. Data set 2. Predicted cumulative confirmed cases ∼Sept 18, 2020, from top to down using Prophet and Neural Networks method of Predict. On the down, from left to right with data set & contact rate and data set only.

Date	$\hat{y}$	$\hat{y}_{lower}$	$\hat{y}_{upper}$
2020-09-14	11827.154428	7680.757057	15751.856303
2020-09-15	11907.049231	7721.053577	15888.511751
2020-09-16	11978.595002	7769.517365	15984.853526
2020-09-17	12051.967485	7776.250955	16102.077092
2020-09-18	12132.562027	7824.092604	16225.629593

Date	P^{β}	P^{β}_{lower}	P^{β}_{upper}	P	P_{lower}	P_{upper}
2020-09-14	7404.458859	7334.148519	7474.769201	12499.239975	12431.730495	12566.749456
2020-09-15	7439.797975	7369.487634	7510.108316	12582.463095	12514.953615	12649.972576
2020-09-16	7475.119671	7404.809330	7545.430012	12665.674270	12598.164790	12733.183751
2020-09-17	7510.423945	7440.113604	7580.734286	12748.868522	12681.359041	12816.378002
2020-09-18	7545.708310	7475.397969	7616.018651	12832.053814	12764.544334	12899.563295

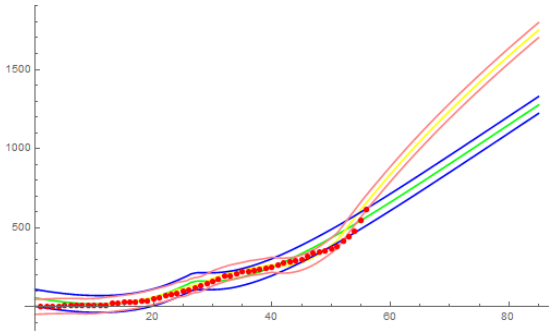

(A) The forecasting is until 2020, May 26.

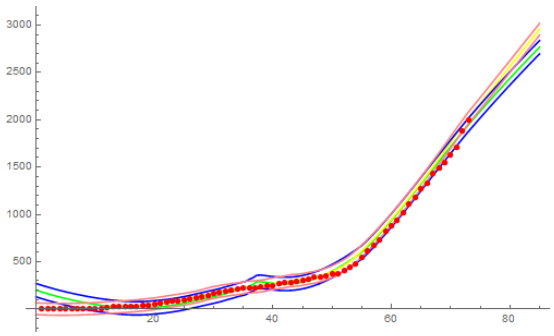

(B) The forecasting is until 2020, May 26.

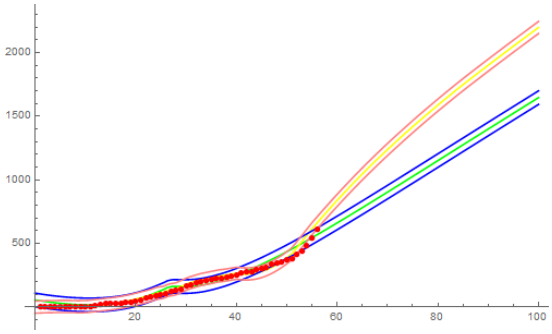

(C) The forecasting is until 2020, June 10.

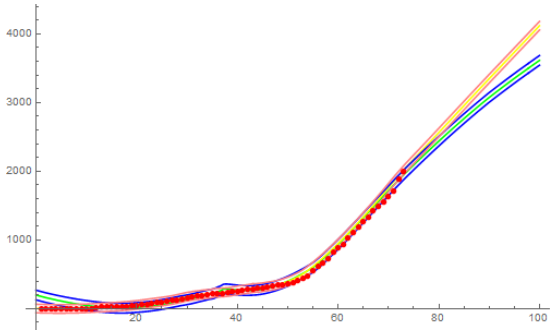

(D) The forecasting is until 2020, June 10.

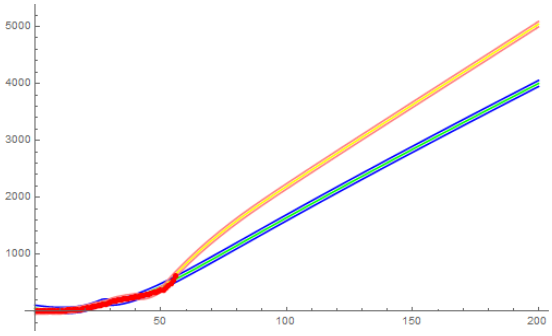

(E) The forecasting is until 2020, September 18.

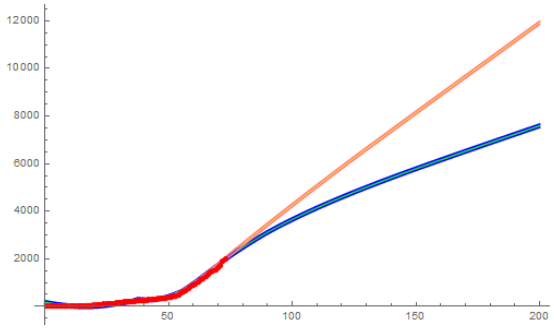

(F) The forecasting is until 2020, September 18.

FIGURE 11. Comparative forecasting, using Neural Networks, of the total number of infected cases. On the abscissa axis the graduations 85, 100 and 200 correspond to the dates 2020, May 26, June 10 and September 18. Forecasting using cumulative data only in yellow curve with confidence interval in orange, using both cumulative and contact rate data in green curve with confidence interval in blue, and data in red dotted. In the left plot using data set 1 and in the right plot using data set 2.

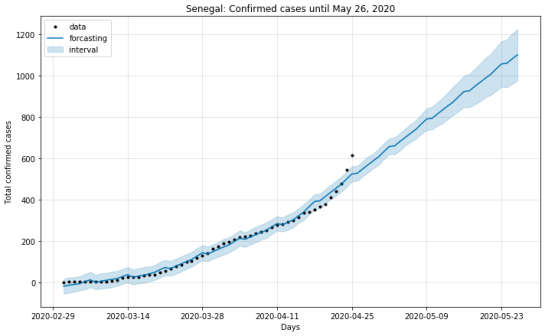

(A) The forecasting is until the date 2020, May 26.

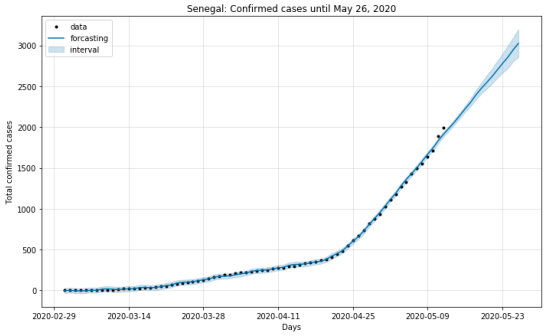

(B) The forecasting is until the date 2020, May 26.

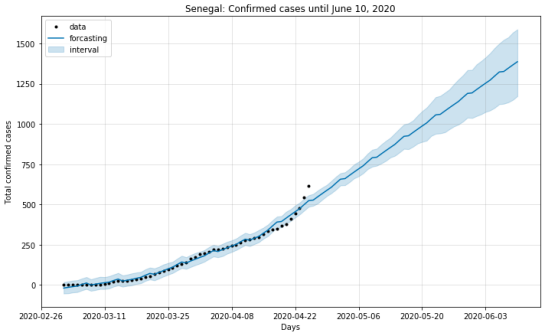

(C) The forecasting is until the date 2020, June 10.

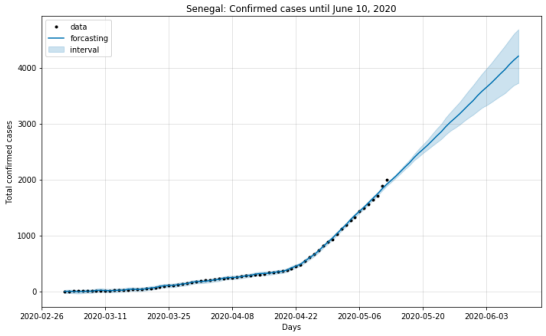

(D) The forecasting is until the date 2020, June 10.

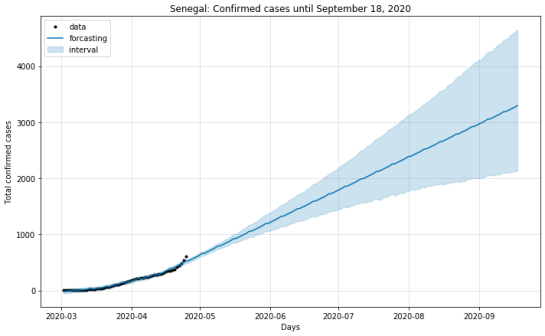

(E) The forecasting is until the date 2020, September 18.

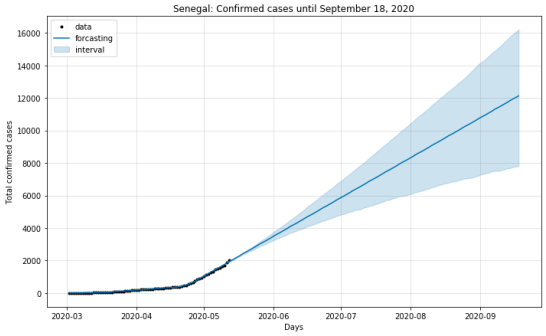

(F) The forecasting is until the date 2020, September 18.

FIGURE 12. Forecasting, using Prophet, of the total number of infected cases until the dates 2020, May 26, June 10 and September 18, from top to down. In left plot using data set 1 and in the right plot using data set 2.

4. Discussion

Analysis of the new trend in the data from March 2 to April 24, 2020 shows a change in the trajectory of the total number of cases. That causes a reduction of the maximum value of the peak compared to what it would have been without the measures taken on March 23, 2020. See figures 6a, 6b, 8b, 8a.

By considering new nationwide measures of Senegal, which we have chosen in this study to fix on the date of May 10, 2020, we note that the maximum value of the peak decreases according to the force of the measures taken. Likewise, the time of the peak is postponed as shown by the parametric plots in figures 6, 7, 8 and 9.

Since the first measures on March 23, 2020, Senegal has laughed at additional measures such as the closing of markets, shops, stores and other public places, with an opening calendar. We have therefore chosen May 10, 2020 as a date from which the additional measures can begin to take effect in reducing contamination.

We see that depending on the strength of these measures, the evolution of the disease can lose its exponential nature or become slower.

The prediction with neural networks and Prophet show an optimistic situation. The forecasting based only on data and those on contact rates show a slow evolution as shown in figures 11 and 12. We see that the curve obtained using the contact rate function in training of the neural networks, goes below that obtained only using the data on the total number of cases.

5. Materials and Methods

5.1. Basic proprieties. Let's set $E = \{(S,I,I_R,I_U) \in \mathbb{R}^4_+ : S+I+I_R+I_U \leq N\}$, N is the initial population. Replacing an initial solution $(S,I,I_R,I_U) \in E$ in the system (1), we obtain:

$$\begin{cases} \dot{S} \leq 0 \\ \dot{I} \geq -\nu I(t) \\ \dot{I_R} \geq -\eta I_R(t) \\ \dot{I_U} \geq -\eta I_U(t) \end{cases} \tag{8}$$

Solving these differential inequalities gives $I(t) \geq K\exp(-\nu t)$, $I_R(t) \geq K\exp(-\eta t)$ and $I_U \geq K\exp(-\eta t)$. Hence $I,\ I_R,\ I_U \geq 0$.

By considering an initial solution with $S = 0$, we get $\dot{S} = 0$. Then $S(t) \geq 0$.

Now, summing the equations of the system (1), we obtain $\dot{S} + \dot{I} + \dot{I_R} + \dot{I_U} \leq -\eta(I_R + I_U) \leq 0$. Then $S + I + I_R + I_U \leq S_0 + I_0 + I_{R0} + I_{U0} \leq N$. Finally (S, I, I_R, I_U) remain in the set E. This implies that E is a positively-invariant set under the flow described by (1). In addition, the model can be considered as being epidemiologically and mathematically well-posed.

Let's set

$$X = \begin{pmatrix} S \\ I \\ I_R \\ I_U \end{pmatrix}, \; f(X(t)) = \begin{pmatrix} -\beta S(t)(I(t) + I_U(t)) \\ \beta S(t)(I(t) + I_U(t)) - \nu I(t) \\ \gamma \nu I(t) - \eta I_R(t) \\ (1-\gamma)\nu I(t) - \eta I_U(t) \end{pmatrix} \text{ and } X_0 = \begin{pmatrix} S_0 \\ I_0 \\ I_{R0} \\ I_{U0} \end{pmatrix} \in E \tag{9}$$

Then the system (1) with initial condition can be rewritten in the following form:

$$\begin{cases} \dot{X} = f(X(t)) \\ X(t_0) = X_0 \end{cases} \tag{10}$$

Theorem 5.1. *The system* (10) *has a unique solution $X(t)$ for $t \geq t_0$.*

Remark 5.1. *The proof of the above theorem come from the Cauchy-Lipschitz theorem and the Fundamental Existence-Uniqueness theorem in* [14]*, since $f \in C^1(E)$.*

Let's set the function $g : \mathbb{R}_+ \times \mathbb{R} \to \mathbb{R}$ such that $g(\beta, X) = f(X)$.

$$g : \begin{array}{rl} \mathbb{R}_+ \times \mathbb{R} & \to \mathbb{R} \\ (\beta, X) & \mapsto f(X) \end{array}, \; \tilde{f}(X) = \begin{cases} g(\beta, X) & \text{if } t \in [t_0, T] \\ g(\beta(\frac{T}{t})^{\delta/p}, X) & \text{if } t > T \end{cases}$$

Then the system (5) can be written in the following form:

$$\begin{cases} \dot{X} = \tilde{f}(X(t)) \\ X(t_0) = X_0 \end{cases} \tag{11}$$

Theorem 5.2. *For any fixed parameters δ and p for $\tilde{\beta}$* (3) *or φ for $\tilde{\beta}$* (4)*, the system* (11) *with $\tilde{\beta}$* (3) *or $\tilde{\beta}$* (4)*, has a unique solution $X(t)$ for $t \geq t_0$.*

Proof of Theorem 5.2. The proof of the existence uniqueness of the system (11) with $\tilde{\beta}$ (3) and $\tilde{\beta}$ (4) are similar. Then, we do this for one.

The function $\tilde{f}$ is piece-wise continuously differentiable in $\mathbb{R}_+ \times E$. Then by using the theorem 5.1, we have the existence of a unique solution $X_1(t)$ on $[t_0, T]$ of the system $\begin{cases} \dot{X} = g(\beta, X(t)) \\ X(t_0) = X_0 \end{cases}$ and for the parameters δ and p fixed, there is a unique solution $X_2(t)$ for $t \geq T$ of the system $\begin{cases} \dot{X} = g(\beta(\frac{T}{t})^{\delta/p}, X(t)) \\ X(T) = X_1(T) \end{cases}$.

Now defining the function $X(t) = \begin{cases} X_1(t) & \text{if } t \in [t_0, T] \\ X_2(t) & \text{if } t > T \end{cases}$, we deduce that $X(t)$ is a unique solution continuous in time of the system (11). □

Remark 5.2. *We can do the same work for the system* (5) *with* $\tilde{\beta}$ *replaced by* $\tilde{\beta}_2$ (6)*. Then for any fixed parameters* δ*,* p *and* ϕ*, the system has a unique solution* $X(t)$ *for* $t \geq t_0$*.*

5.2. Disease Free Equilibrium. The unique equilibrium of the model (1) is the canonical DFE given by $(S_0, 0, 0, 0)$.

5.3. Parameters estimation. The estimation of the parameters of the model (1) is done by using techniques in [9], [3]. We fit the cumulative data with an exponential function $TNI(t) = b\exp(ct) - a$. In addition, we assume that the cumulative function can be given in integral form as $TNI(t) = \gamma\nu \int_{t_0}^{t} I(s)ds$.

Then $TNI(t_0) = TNI_0 = b\exp(ct_0) - a = 0$. Thus, we obtain $t_0 = \dfrac{\ln(a) - \ln(b)}{c}$.

Also we have:

$$I(t) = T\dot{N}I(t) = bc\exp(ct). \tag{12}$$

Then $I(t_0) = \dfrac{bc}{\gamma\nu}\exp(ct_0) = \dfrac{ac}{\gamma\nu} = I_0$ and $\dfrac{I(t)}{I(t_0)} = \exp(c(t - t_0))$. Hence, we obtain

$$I(t) = I(t_0)\exp(c(t - t_0)), \tag{13}$$

then $\dot{I}(t) = cI(t)$ and $\dot{I}(t_0) = cI(t_0)$.

Let's set δ_1 and δ_2 such that $I_1 = \delta_1 I$ and $I_2 = \delta_2 I$. Then replacing in the second an third

equation of the following system:

$$\left\{\begin{array}{lcl} \dot{I} & = & \beta\, S(I+I_U) - \nu\, I \\ \dot{I}_R & = & \gamma\nu\, I - \eta\, I_R \\ \dot{I}_U & = & (1-\gamma)\nu\, I - \eta\, I_U, \end{array}\right. \tag{14}$$

we obtain

$$\delta_1 = \frac{\gamma\nu}{c+\eta} = \frac{I_{R0}}{I_0} \tag{15}$$

$$\delta_2 = \frac{(1-\gamma)\nu}{c+\eta} = \frac{I_{U0}}{I_0} \tag{16}$$

Then introducing (16) in the first equation of (14), we obtain:

$$c+\nu = \beta\, S_0\,(1+\delta_2).$$

Hence

$$\beta = \frac{c+\nu}{S_0\,(1+\delta_2)}. \tag{17}$$

Replacing (16) in (17), we obtain:

$$\beta = \frac{(c+\nu)(c+\eta)}{S_0\,(c+\eta+(1-\gamma)\nu)}. \tag{18}$$

5.4. The basic reproductive number $\mathscr{R}_0$. To compute the $\mathscr{R}_0$, we use [17]. We consider the linearized infected equations at the Disease Free Equilibrium (DFE) $(S_0,0,0,0,0,0)$, in the system (2):

$$\left\{\begin{array}{l} \dfrac{dI}{dt} = \beta S_0(I(t)+I_U(t)) - \nu I(t) \\ \\ \dfrac{dI_U}{dt} = (1-\gamma)\nu I(t) - \eta I_U(t) \end{array}\right. \tag{19}$$

Extracting the matrix:

$$M = \begin{bmatrix} \beta S_0 - \nu & \beta S_0 \\ (1-\gamma)\nu & -\eta \end{bmatrix}$$

$$= \begin{bmatrix} \beta S_0 & \beta S_0 \\ (1-\gamma)\nu & 0 \end{bmatrix} - \begin{bmatrix} \nu & 0 \\ 0 & \eta \end{bmatrix}$$

Then the next generation is given by:

$$FV^{-1} = \begin{bmatrix} \beta S_0/\nu & \beta S_0/\eta \\ (1-\gamma) & 0 \end{bmatrix}$$

Finally the spectral radius $\rho(FV^{-1})$ gives:

$$\mathscr{R}_0 = \frac{\beta S_0}{\nu}(1 + \frac{(1-\gamma)\nu}{\eta}). \tag{20}$$

6. Conclusion and Perspectives

In this paper, we have analyzed the impact of anti-pandemic measures in Senegal. First, we used techniques of fitting function to the data of the total number of cases. The choice of the data fit function is crucial for the results since it allows the estimation of the parameters of the compartmental model used. In a second work, we use machine learning tools to also predict the future evolution of the pandemic in Senegal. Also, we have integrated the effects of the measures into the prediction.

Depending on the measures taken, the pandemic's trajectory may become slower or lose its exponential nature. It would be interesting, in the following, to use other functions of a slow nature like the logistical function to fit data and thus obtain different results. A stochastic study using Brownian motions applied to the SIRU compartmental model would also be interesting.

Acknowledgement

The authors thanks the Non Linear Analysis, Geometry and Applications (NLAGA) Project for supporting this work.

CONFLICT OF INTERESTS

The author(s) declare that there is no conflict of interests.

REFERENCES

[1] E. Alpaydin, Introduction to Machine Learning 2nd ed, 584. Adaptive Computation and Machine Learning, MIT Press, 2010.

[2] R. M. Anderson and R. M. May, Infectious Diseases of Humans, 768. Oxford University Press, Oxford, 1992.

[3] M.A.M.T. Baldé, Fitting SIR model to COVID-19 pandemic data and comparative forecasting with machine learning, medRxiv 2020.04.26.20081042; https://doi.org/10.1101/2020.04.26.20081042. 2020.

[4] I. Goodfellow, Y. Bengio and A. Courville, Deep Learning, MIT Press. http://www.deeplearningbook.org, 2016.

[5] J. Heaton, AIFH Volume 3: Deep Learning and Neural Networks, Heaton Research, Inc, 268. Tracy Heaton, 2015.

[6] H. W. Hethcote, The Mathematics of Infectious Diseases, SIAM Rev. 42 (4) (2000), 599–653.

[7] H.P. Langtangen, G.K. Pedersen, Scaling of Differential Equations, Springer International Publishing, Cham, 2016.

[8] F. Di Lauro, I.Z. Kissy, and J.C. Miller, The timing of one-shot interventions for epidemic control, medRxiv 2020.03.02.20030007; https://doi.org/10.1101/2020.03.02.20030007, 2020

[9] Z. Liu, P. Magal,O. Seydi, G. Webb, Understanding Unreported Cases in the 2019-Ncov Epidemic Outbreak in Wuhan, China, and the Importance of Major Public Health Interventions, SSRN: https://ssrn.com/abstract=3530969 or http://dx.doi.org/10.2139/ssrn.3530969. 2020.

[10] Z. Liu, P. Magal, O. Seydi, G. Webb, Predicting the cumulative number of cases for the COVID-19 epidemic in China from early data, Math. Biosci. Eng. 17 (4) (2020), 3040-3051.

[11] B.M. Ndiaye, L. Tendeng, D. Seck, Analysis of the COVID-19 pandemic by SIR model and machine learning technics for forecasting, ArXiv:2004.01574 [Math, q-Bio, Stat]. (2020). http://arxiv.org/abs/2004.01574, 2020.

[12] B.M. Ndiaye, L. Tendeng, D. Seck, Comparative prediction of confirmed cases with COVID-19 pandemic by machine learning, deterministic and stochastic SIR models, ArXiv:2004.13489 [Math, q-Bio, Stat]. (2020). http://arxiv.org/abs/2004.13489, 2020.

[13] M.E.J. Newman, Networks An Introduction, Oxford University Press, Oxford, 394. (2010).

[14] L. Perko, Differential equations and dynamical systems, Springer-Verlag, New-York, 1991.

[15] Prophet: Automatic Forecasting Procedure, avalailable in https://facebook.github.io/prophet/docs/ or https://github.com/facebook/prophet.

[16] Python Software Foundation. Python Language Reference, version 2.7. Available at http://www.python.org.

[17] P. Van den Driessche, J. Watmough, Reproduction numbers and subthreshold endemic equilibria for compartmental models of disease transmission, Math. Biosci. 180 (2002), 29-48.

[18] Wolfram Mathematica, https://www.wolfram.com/mathematica/?source=nav.